

ORIGINAL ARTICLE

Remotely excited Raman optical activity using chiral plasmon propagation in Ag nanowires

Mengtao Sun^{1*}, Zhenglong Zhang^{1*}, Peijie Wang², Qiang Li¹, Fengcai Ma³ and Hongxing Xu¹

We experimentally investigated remotely excited Raman optical activity (ROA) using propagating surface plasmons in chiral Ag nanowires. Using chiral fmoc-glycyl-glycine-OH (FGGO) molecules, we first studied the local surface plasmon-enhanced ROA. We found that the Raman intensity can be excited by left- and right-circularly polarized lights and that the circular intensity difference (CID) can be significantly enhanced. Second, by selecting vibrational modes with large Raman and ROA intensities that are not influenced by chemical enhancements, we studied remotely excited ROA imaging and the CID of FGGO molecules by propagating a plasmonic waveguide using Ag chiral nanostructures. When laser light was radiated on one of the Ag terminals, the measured CID of the FGGO at the other terminal showed little change compared to the local excited CID. Meanwhile, when the laser light was radiated on the Ag nanowires (not on the terminals) and was coupled to the nearby nanoantenna, the CID of the ROA could be manipulated by altering the coupling angle between the Ag nanowires. To directly demonstrate the propagation of ROA along the nanowire and its remote detection, we also measured the remotely excited ROA spectra. Our experimental method has the potential to remotely determine the chirality of molecular structures and the absolute configuration or conformation of a chiral live cell.

Light: Science & Applications (2013) 2, e112; doi:10.1038/lisa.2013.68; published online 22 November 2013

Keywords: Ag nanowires; chiral plasmons; plasmon propagation; Raman optical activity; remote excitation

INTRODUCTION

Raman optical activity (ROA)^{1–3} results in differences in the Raman spectra excited by right- and left-circularly polarized light; this activity is extremely sensitive to the chirality of the molecular structure^{4–6} and can reveal the absolute molecular configuration⁵ or conformation.⁶ Several excellent reviews of ROA have been reported.^{7–9} The dimensionless circular intensity difference (CID) introduced by Barron and Buckingham¹ provides an experimental observable of this phenomenon:

$$\Delta = \frac{|I_L - I_R|}{|I_L + I_R|} \quad (1)$$

where I_R and I_L are the Raman scattering intensities of right- and left-circularly polarized light, respectively. Although chiral-sensitive vibrational spectroscopy has become increasingly popular in biological applications, this approach has an obvious flaw that is difficult to overcome: the ROA scattering intensities are 10^{-3} – 10^{-5} times the intensities of the parent Raman scattering. Due to the low intensity of ROA, this technique has certain limitations and requires higher sample concentrations and longer data collection periods.

The intrinsic weakness of ROA can be resolved by utilizing surface plasmon enhancement.^{10–17} The local electric field and field gradients generated by plasmon resonance can significantly enhance the ROA

and CID.⁹ Surface-enhanced ROA is attributed to the coupling between the electric dipole and the electric quadrupole terms in the process of Raman scattering.¹⁶ The quadrupole transitions can only be significantly excited in an oriented molecule close to the metallic substrate; under far-field excitations, the transitions are weak.

In general, the influence of chemical enhancement is difficult to distinguish in surface-enhanced ROA. Some vibrational modes are strongly influenced by chemical enhancements, while for other modes, chemical enhancements can be ruled out based on the characterization of selective chemical enhancement. Thus, we must carefully select vibrational modes that exhibit both strong Raman and CID intensities for which there is no influence of chemical enhancement.

The propagation of a surface plasmon polariton along metal nanowires enables the incident light to transfer through a subdiffraction-limit nanowire over micrometer-scale distances.¹⁸ This unique property of surface plasmons enables the achievement of miniaturized photonic nanowires and high-resolution spectroscopy and microscopy. Remotely excited surface-enhanced Raman scattering (SERS) produced by means of a propagating surface plasmon in Ag or Au nanowires has been experimentally studied.^{19–21} Compared to local SERS techniques that excite targets directly, the remote excitation method can avoid specimen damage caused by the laser, which may be critical in some cases, for example, in intercellular chiral live cells.

¹Beijing National Laboratory for Condensed Matter Physics, Institute of Physics, Chinese Academy of Sciences, Beijing 100190, China; ²Department of Physics, Capital Normal University, Beijing 100048, China and ³Department of Physics, Liaoning University, Shenyang 110036, China

*These authors contributed equally to this work.

Correspondence: Professor MT Sun, Beijing National Laboratory for Condensed Matter Physics, Institute of Physics, Chinese Academy of Sciences, PO Box 603-146, Beijing 100190, China

E-mail: mtsun@iphy.ac.cn

Received 22 March 2013; revised 20 July 2013; accepted 23 July 2013

Further, chiral plasmonic nanostructures²² can be used to manipulate and enhance the CID of intrinsic chiral molecules. Thus, it is desirable to design plasmonic nanostructures for local and remote chiral sensing.²³

In this communication, we report an experimental realization of remotely excited ROA *via* chiral plasmons propagating on Ag nanowires. To directly demonstrate the propagation of ROA along a nanowire and its remote detection, we also measured the remotely excited ROA spectra. This approach has the potential to remotely determine the chirality of molecular structures and the absolute configuration or conformation of chiral living cells.

MATERIALS AND METHODS

Fmoc-glycyl-glycine-OH (FGGO) was obtained from Aldrich Chemical (China) Co. and was used as received. The Raman and ROA spectra (Figure 1) were collected using the backscattering SCP Biotools μ -ChiralRAMAN-2X. The laser light had a wavelength of 532 nm,²⁴ and a power of 300 mW was radiated on the sample. The total collection time was 4 h.

Single crystalline Ag nanowires were synthesized using chemical methods.²⁵ High-resolution scanning electron microscopy (SEM) images were acquired at a voltage of 10 kV. The Ag nanowires were mixed with FGGO ethanol solution (0.04 M) for 24 h and were then dropped on a glass substrate. To examine the influence of the substrate on the shift in the Raman frequencies for SERS, the local SERS was measured with linearly polarized light excited at 632.8 nm, using a Leica microscope installed with a confocal Raman spectroscopic instrument (Invia; Renishaw, UK) with a 100 \times objective and a numerical aperture of 0.85. Then, local and remote Raman images of the molecular vibrational mode at 1593 cm⁻¹ were obtained using right- and left-circularly polarized light, respectively. This vibrational mode exhibits large Raman ROA intensities and is not influenced by chemical enhancements. The optical images were recorded using a TE-cooled CCD detector installed on the microscope. The Raman images were remotely measured. Laser light at 632.8 nm (power of approximately

7 mW) was radiated on the crossing point (point a in Figure 2a) using left- and right-circularly polarized light, respectively, and the Raman signals were measured at the remote terminals of the nanowires (points b, c and d in Figure 2a). This method of measuring a single Raman mode propagating along a nanowire has been described in detail in Refs. 19, 20, 26 and 27; this approach is generally called Raman imaging in SERS. Finally, using Equation (1), local and remote surface plasmon-enhanced ROA imaging can be obtained. To directly demonstrate the propagation of the ROA along the nanowire and its remote detection, we also measured the remotely excited ROA spectra.

We fabricated a metal-insulator-semiconductor nanowire plasmonic waveguide system consisting of a wet-chemically grown Ag wire, which was then covered by Al₂O₃ films of varying thickness using an atomic layer deposition (ALD) system (Savannah-100; Cambridge NanoTech, USA) to achieve a well-defined thickness. Subsequently, the sample was spin-coated with highly luminescent CdSe/ZnS Organic Quantum Dots (Qdot 655; Invitrogen, China).

Theoretical simulations were performed using Gaussian 09.²⁸ The geometry of FGGO at the ground state was optimized at the level of density functional theory,²⁹ the B3LYP functional,³⁰ and the 6-311+g(2d,p) basis set. Using the optimized ground state geometry of FGGO, the Raman and ROA spectra of FGGO were then simulated.

RESULTS AND DISCUSSION

The experimental Raman and ROA spectra of FGGO are shown in Figure 1a and 1b. The highest intensities for both spectra appear at 1607 cm⁻¹, with a CID value of $\Delta=0.57\%$. The vibrational mode of this peak is shown in Figure 1c, which provides the best candidate for studying the remote excitation ROA using chiral plasmon propagation in Ag nanowires. For the vibration mode at 1607 cm⁻¹, both the Raman and CID intensities are at their maxima, based on the experimental spectra shown in Figure 1. This vibrational mode corresponds to the symmetric vibration of ¹H-fluorenyl, and there are no O or N atoms in this group. In general, O and N atoms directly interact with metal, and thus, vibrational modes for groups including these atoms

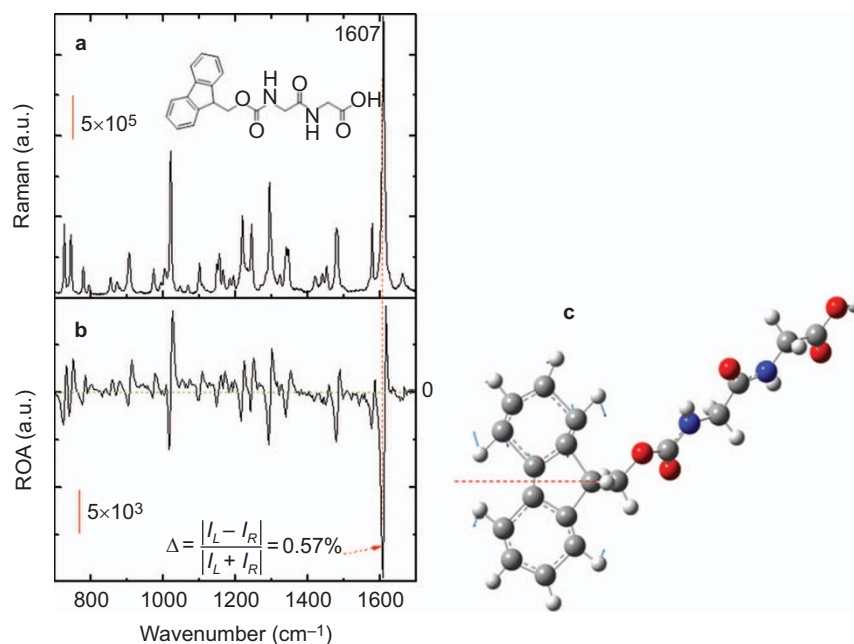


Figure 1 Experimental Raman and ROA spectra and the vibrational mode of FGGO at 1607 cm⁻¹. (a) Raman spectrum. (b) ROA spectrum. (c) Vibrational mode of FGGO at 1607 cm⁻¹. FGGO, fmoc-glycyl-glycine-OH; ROA, Raman optical activity.

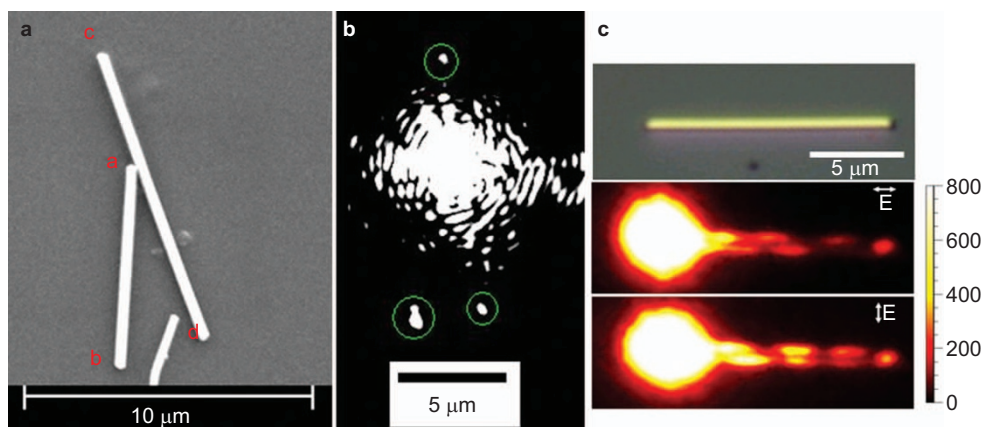


Figure 2 The structure of the Ag nanowires and the propagation of surface plasmons in the Ag nanowires. (a) Structure of the Ag nanowires. (b) Surface plasmons propagating in the Ag nanowires. (c) Optical image of a single nanowire and evidence of the chiral propagation of surface plasmons in the Ag nanowires. The chirality can be manipulated by the polarization of the laser.

are usually strongly influenced by chemical enhancements. In this case, there is no direct interaction between the group and the metal, and hence, there is no chemical enhancement for this vibrational mode. The assignments of the other vibrational modes with relatively strong Raman and CID intensities are given in Supplementary Fig. S1.

A glass substrate was used in the experiments. An SEM image of the Ag nanowires is shown in Figure 2a; the crossing angle between the nanowires was found to be approximately 20°. Figure 2b demonstrates the propagation of plasmons in the Ag nanowires, and the light can be clearly observed at the terminals of the nanowires. To reveal the chiral propagation of the surface plasmons in the nanowire, the simplest nanostructure (a single nanowire) was used. Figure 2c shows an optical image of chiral surface plasmons propagating along a single nanowire. The degree of this type of chiral propagation can be manipulated *via* the polarization of the laser.

The SERS spectrum of locally excited FGGO at the crossing point of the Ag nanowires is shown in Supplementary Fig. S2 for linearly polarized light. The vibrational mode at 1607 cm^{-1} in Figure 1a was shifted to 1593 cm^{-1} due to the interaction between the FGGO and the Ag nanowires. Finally, local and remote Raman images of FGGO at 1593 cm^{-1} , excited by left- and right-circularly polarized light, are shown in Figure 3a and 3b, respectively. As discussed above, this vibrational mode exhibits large Raman and ROA intensities, without the influence of chemical enhancement. Due to the chiral properties of the nanowire structure and the propagating surface plasmon, we observed different local and remote intensities of the Raman imaging at 1593 cm^{-1} . The Raman intensities at these four points are significantly stronger when excited by the left circular polarization in comparison to the right circular polarization. Using Equation (1), the fitted CIDs at four points were obtained, as shown in Figure 3c. The

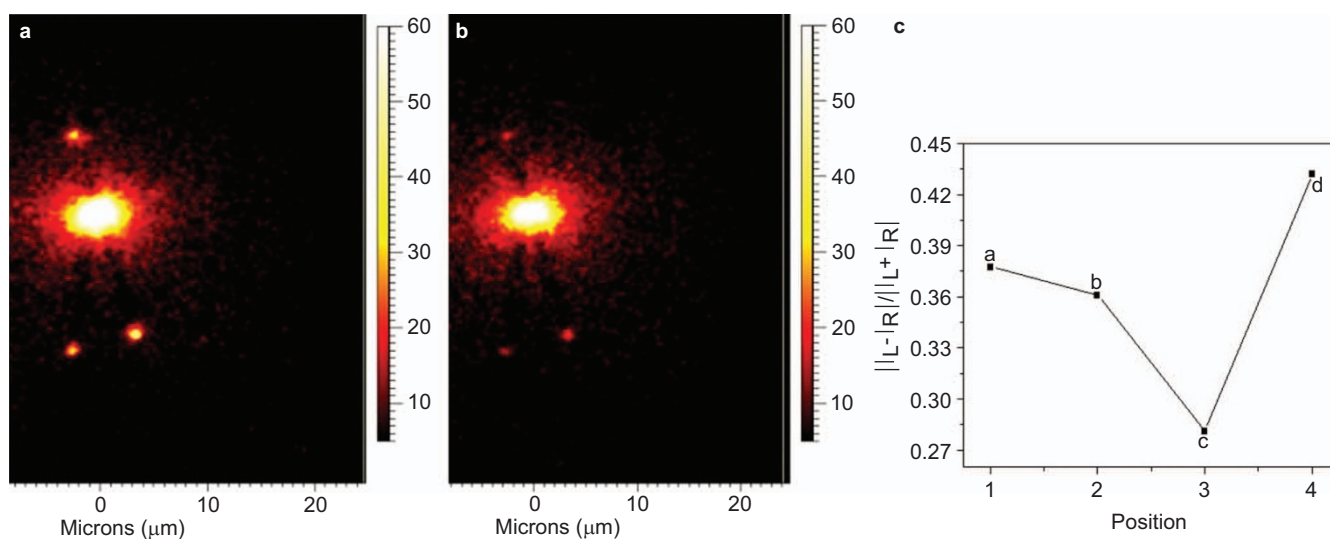


Figure 3 Imaging of the Raman peak of FGGO at 1593 cm^{-1} , excited by circular polarization, and the fitted CIDs at four different points. (a) Results for left circular polarization. (b) Results for right circular polarization. (c) The fitted CIDs at four points of the nanostructure. CID, circular intensity difference; FGGO, fmc-glycyl-glycine-OH.

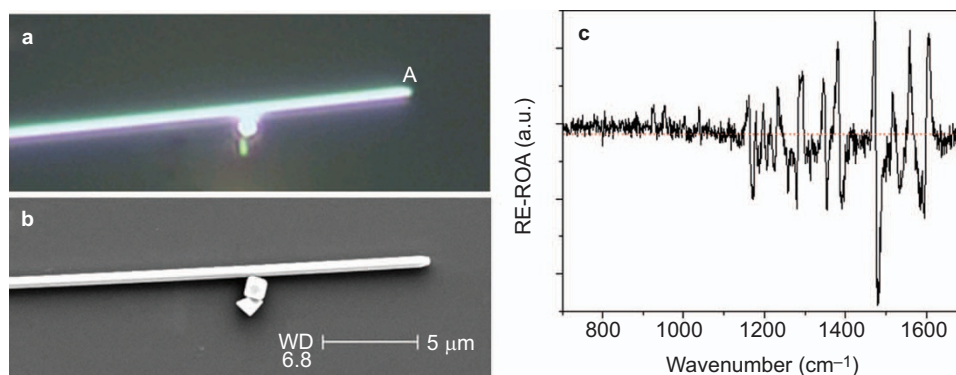


Figure 4 The nanostructure of the nanowire and the nanoparticle and the remotely excited ROA. (a) Optical imaging. (b) SEM imaging of the nanostructure of the nanowire and the nanoparticle. (c) The remotely excited ROA. ROA, Raman optical activity; SEM, scanning electron microscopy.

CIDs are significantly enhanced compared to the intrinsic molecular powder. Furthermore, the three CIDs at the three terminals of the Ag nanowires are also significantly different.

A comparison of the CID at crossing point A (the point at which the laser is radiated) to that at point B (the remote terminal of the same Ag nanowire) shows that the change in the CID is small. Therefore, the chiralities of both the propagating surface plasmon and the molecule do not change from one terminal to the other. In contrast, when the plasmon is coupled into the Ag nanowire at some point along the Ag nanowire close to the nanoantenna, the CIDs at the two remote terminals are very different and can be manipulated by the chiral nanostructure. In our case, the coupling angle between two Ag nanowires, the morphology of the Ag terminals, the distance of the coupling, *etc.*, can be used to manipulate the chirality of the propagating surface plasmon.^{31,32} The changing chirality of the propagating surface plasmon can further change the molecular chirality and thus alter the CID value. In our fabricated nanostructure, when the crossing angle was less than 90°, the CID increased; when the crossing angle was larger than 90°, the CID decreased. Thus, we experimentally imaged remotely excited ROA using chiral plasmon propagation in Ag nanowires, and this method has the potential to remotely determine molecular chirality or the absolute configuration or conformation of a chiral living cell.

To directly demonstrate the propagation of ROA along the nanowire and its remote detection, we also measured the remotely excited ROA spectra (Figure 4). Figure 4a and 4b show optical and SEM images of the Ag nanowire and a nanoparticle as the nanoantenna for the electromagnetic enhancement. The remotely excited Raman spectra were obtained using left and right polarized light (Supplementary Fig. S3). The laser was radiated on terminal A, and the signals were collected from the crossing point between the nanoparticle and the nanowire. Figure 4c displays the remotely excited ROA spectrum resulting from the propagating plasmonic waveguide, which is significantly different from the molecular ROA shown in Figure 1b. For some of the Raman peaks in Figure 4c, the signals were stronger than that at 1593 cm⁻¹, which arose from chemical enhancements or the chiral nanostructures. It is known that chiral nanostructures can produce a chiral propagating plasmonic waveguide, which may also selectively enhance certain Raman peaks in the remotely excited ROA. A detailed analysis of the relationship among the ROA, the chemical mechanism and the chiral propagating plasmonic waveguide is currently being pursued.

CONCLUSIONS

We experimentally achieved remotely excited ROA imaging by selecting a single vibrational mode propagating along a nanowire, using a chiral plasmon propagating in Ag nanowires. The local and remote Raman intensity of FGGO at 1593 cm⁻¹ were significantly enhanced when excited by left- and right-circularly polarized light. This vibrational mode exhibited large Raman and ROA intensities, without the influence of chemical enhancements. Furthermore, the local and remote CIDs, which were also significantly increased, were fitted and can be successfully manipulated by the nanostructure of the Ag nanowires. To directly demonstrate the propagation of ROA along the nanowire and its remote detection, we also measured the remotely excited ROA spectra. This work may be potentially utilized to remotely investigate the chirality of molecular structures, as well as the absolute configuration or conformation of chiral living cells.

ACKNOWLEDGMENTS

This work was supported by the National Natural Science Foundation of China (11374353 and 11274149) and the Program of Shenyang Key Laboratory of Optoelectronic Materials and Technology (F12-254-1-00).

- Barron LD, Buckingham AD. Rayleigh and Raman scattering from optically active molecules. *Mol Phys* 1971; **20**: 1111–1119.
- Barron LD, Bogaard MP, Buckingham AD. Raman scattering of circularly polarized light by optically active molecules. *J Am Chem Soc* 1973; **95**: 603–605.
- Hug W, Kint S, Bailey GF, Scherer JR. Raman circular intensity differential spectroscopy. Spectra of (2)-a-pinene and (1)-a-phenylethylamine. *J Am Chem Soc* 1975; **97**: 5589–5590.
- Sebestik J, Bour P. Raman optical activity of methyloxirane gas and liquid. *J Phys Chem Lett* 2011; **2**: 498–502.
- Hopmann KH, Sebestik J, Novotna J, Stensen W, Urbanova M *et al*. Determining the absolute configuration of two marine compounds using vibrational chiroptical spectroscopy. *J Org Chem* 2012; **77**: 858–869.
- Haesler J, Schindelholz I, Riguef E, Bochet CG, Hug W. Absolute configuration of chirally deuterated neopentane. *Nature* 2007; **446**: 526–529.
- Barron LD, Hecht L, McColl IH, Blanch EW. Raman optical activity comes of age. *Mol Phys* 2004; **102**: 731–744.
- Nafie LA. Vibrational optical activity in focus. *Appl Spectrosc* 1996; **50**: A12.
- Pecul M. New applications and challenges for computational ROA spectroscopy. *Chirality* 2009; **21**: E98–E104.
- Efrima S. The effect of large electric field gradients on the Raman optical activity of molecules adsorbed on metal surfaces. *Chem Phys Lett* 1983; **102**: 79–82.
- Efrima S. Raman optical activity of molecules adsorbed on metal surfaces: theory. *J Chem Phys* 1985; **83**: 1356.
- Etchegoin PG, Galloway C, Le Ru EC. Polarization-dependent effects in surface-enhanced Raman scattering (SERS). *Phys Chem Chem Phys* 2006; **8**: 2624–2648.
- Janesko BG, Scuseria GE. Surface enhanced Raman optical activity of molecules on orientationally averaged substrates: theory of electromagnetic effects. *J Chem Phys* 2006; **125**: 124704.

- 14 Kneipp H, Kneipp J, Kneipp K. Surface-enhanced Raman optical activity on adenine in silver colloidal solution. *Anal Chem* 2006; **78**: 1363–1366.
- 15 Abdalia S, Blanch EW. Surface enhanced Raman optical activity (SEROA). *Chem Soc Rev* 2008; **37**: 980–992.
- 16 Yang N, Tang Y, Cohen AE. Spectroscopy in sculpted fields. *Nano Today* 2009; **4**: 269–279.
- 17 Novak V, Sebestik J, Bour P. theoretical modeling of the surface-enhanced Raman optical activity. *J Chem Theory Comput* 2012; **8**: 1714–1720.
- 18 Dickson RM, Lyon LA. Unidirectional plasmon propagation in metallic nanowires. *J Phys Chem B* 2000; **104**: 6095–6098.
- 19 Fang Y, Wei H, Hao F, Nordlander P, Xu HX. Remote-excitation surface-enhanced Raman scattering using propagating Ag nanowire plasmons. *Nano Lett* 2009; **9**: 2049–2053.
- 20 Huang Y, Fang Y, Sun MT. Remote excitation of surface-enhanced Raman scattering on single Au nanowire with quasi-spherical termini. *J Phys Chem C* 2011; **115**: 3558–3561.
- 21 Lal S, Hafner JH, Halas NJ, Link S, Nordlander P. Noble metal nanowires: from plasmon waveguides to passive and active devices. *Acc Chem Res* 2012; **45**: 1887–1895.
- 22 Helgert C, Pshenay-Severin E, Falkner M, Menzel C, Rockstuhl C *et al*. Chiral metamaterial composed of three-dimensional plasmonic nanostructures. *Nano Lett* 2011; **11**: 4400–4404.
- 23 Schaferling M, Dregely D, Hentschel M, Giessen H. Tailoring enhanced optical chirality: design principles for chiral plasmonic nanostructures. *Phys Rev X* 2012; **2**: 031010.
- 24 Hug W, Hangartner G. A novel high-throughput Raman spectrometer for polarization difference measurements. *J Raman Spectrosc* 1999; **30**: 841–852.
- 25 Sun Y, Xia YN. Large-scale synthesis of uniform silver nanowires through a soft, self-seeding, polyol process. *Adv Mater* 2002; **14**: 833–837.
- 26 Sun M, Hou Y, Li Z, Liu L, Xu H. Remote excitation polarization-dependent surface photochemical reaction by plasmonic waveguide. *Plasmonics* 2011; **6**: 681–687.
- 27 Chandrasekhar N, Mohiddon M, Chandrasekar R. Organic submicro tubular optical waveguides: self-assembly, diverse geometries, efficiency, and remote sensing properties. *Adv Opt Mater* 2013; **1**: 305–311.
- 28 Frisch MJ, Trucks GW, Schlegel HB, Scuseria GE, Robb MA *et al*. *Gaussian 09, Revision A.02*. Wallingford, CT: Gaussian, Inc.; 2009.
- 29 Hohenberg P, Kohn W. Inhomogeneous electron gas. *Phys Rev* 1964; **136**: B864–B874.
- 30 Lee C, Yang W, Parr RG. Development of the Colle–Salvetti correlation energy formula into a functional of the electron density. *Phys Rev B* 1988; **37**: 785–789.
- 31 Fang YR, Li ZP, Huang YZ, Zhang SP, Nordlander P *et al*. Branched silver nanowires as controllable plasmon routers. *Nano Lett* 2010; **10**: 1950–1954.
- 32 Zhang S, Wei H, Bao K, Hakanson U, Halas NJ *et al*. Chiral surface plasmon polaritons on metallic nanowires. *Phys Rev Lett* 2011; **107**: 096801.



This work is licensed under a Creative Commons Attribution-NonCommercial-ShareAlike 3.0 Unported license. To view a copy of this license, visit <http://creativecommons.org/licenses/by-nc-sa/3.0>

Supplementary Information for this article can be found on *Light: Science & Applications*' website (<http://www.nature.com/lisa/>).